Int J Min & Geo-Eng (IJMGE), Vol. 47, No. 1, Jun. 2013, pp. 81-90

A 3D elasto-plastic FEM program developed for reservoir Geomechanics simulations: Introduction and case studies

Amin Chamani*, Vamegh Rasouli

Department of Petroleum Engineering, Curtin University, ARRC Building, 26 Dick Perry Avenue, Kensington, WA, 6151, Australia.

Received 19 April 2013; Received in revised form 8 June 2013; accepted 15 Jun 2013

Abstract

The development of yielded or failure zone due to an engineering construction is a subject of study in different disciplines. In Petroleum engineering, depletion from and injection of gas into a porous rock can cause development of a yield zone around the reservoir. Studying this phenomenon requires elasto-plastic analysis of geomaterial, in this case the porous rocks. In this study, which is a continuation of a previous study investigating the elastic behaviour of geomaterial, the elasto-plastic responses of geomaterial were studied. A 3D finite element code (FEM) was developed, which can consider different constitutive models. The code features were explained and some case studies were presented to validate the output results of the code. The numerical model was, then, applied to study the development of the plastic zone around a horizontal porous formation subjected to the injection of gas. The model is described in detail and the results are presented. It was observed that by reducing the cohesion of rocks the extension of the plastic zone increased. Comparing to the elastic model, the ability to estimate the extension of the yield and failure zone is the main advantage of an elasto-plastic model.

Keywords: elasto-plastic, FEM, gas injection, plastic zone, porous reservoir.

1. Introduction

Development of plastic zones in porous materials such as soils and rocks, due to an Engineering activity, is a topic of study by many researchers [1]. An example of this research interest is production from a porous reservoir formation or injection into a depleted reservoir for underground storage purposes. The permanent deformation as a result of plastic deformation is irrecoverable, contrary to elastic behaviour if the material is unloaded. The plastic zone represents the extent of the yield of the geomaterial and can be mathematically determined using appropriate constitutive models of plasticity theory [1]. The plastic shear failure could be characterised using Mohr-Coulomb type plasticity constitutive models [2]. Drucker-Prager constitutive model, for example, is also used to determine the plastic zone, due to gas injection into a reservoir formation, which was considered in this study. While both constitutive models are pressure sensitive, the Drucker-Prager model has no singularities and, therefore, is a superior model in this regard. This assumption has been supported by different studies, some of which are discussed here.

Fredrich and Fossum (2002) carried out several case studies using elsato-plastic and viscoplastic constitutive models [3]. They discussed the advantages of continuous surface yielding criterion against traditional cap plasticity models, suggesting that the traditional cap plasticity models have indeterminacy at the point of intersection between shear failure surfaces and hardening cap surface. They further argued that the horizontal tangency of cap hardening surface at the intersection point makes it impossible that the model dilatants before final failure. The continuous surface yielding criteria have not these two disadvantages. Fredrich and Fossum (2002) discussed the effects of production and reservoir depletion on the surrounding rocks, surface subsidence and casing damages [3]. They also performed several case studies using the new continuous surface elasto-plastic models for geomaterial. They estimated the pore pressure using the black-oil model reservoir simulator which was used as the input into the geomechanical model in the form of external loads. Fredrich and Fossum (2002) considered a highly porous diatomaceous formation (a porosity of 45%) located in San Joaquin Basin,

* Corresponding author. Phone: +61892661341, Fax: +61892667063, Email: aminchamani@gmail.com

named Belridge diatomite, and Lost Hill fields where numerous casing damage had been reported [3]. They studied two sections in Belridge Diatomite and one at the Lost Hill field using three-dimensional nonlinear finite element code JAS3D. The results of their modelling revealed that the sliding surface and bedding surface between reservoir and upper formations are the main sources for large horizontal deformation of casing. They also reported that the horizontal displacement is negligible in the first 10 years while production switches to waterflood processes and injection, which shows high shear displacement in the sample well. The results also indicated the tendency of rotation of principle stresses in the field during the course of production, as the minimum principle stress rotates from horizontal to vertical direction.

Minkoff *et al*. (2003) described comprehensively the advantages and disadvantages of fully coupled, loosely coupled and one-way coupled methods between fluid flow and geomechanical equations [4]. Despite the perfectness of fully coupled models, they stated that it is extremely hard to set up the set of simultaneous equations for multiphase flow and nonlinear geomechanical behaviour. However, the one-way coupled method does not possess this perfectness of simultaneous solution of fluid flow and geomechanical set of equations, but the method makes it easier to use advanced and sophisticated fluid flow and geomechanics code to handle the problem. This allows capturing features in advanced problems such as multiphase fluid flow or nonlinear elasto-plastic behaviour of geomaterial. They argued that the loosely coupled method, in between the other two way of coupling, enhances the capability of one-way coupling method, since it allows the updated data transfer between two simulators in order to increase the degree of coupling of the solution.

Nevertheless, the loosely coupled method permits the use of highly progressed and advanced simulators, as they run independently. Using the loosely coupled method, they coupled two advanced simulators of IPARS as a reservoir simulator that is capable of handling multiphase flow and faults and JAS3D, an advanced geomechanics simulator that handles nonlinear complicated constitutive models for geomaterial. In these coupled programs, pore pressure is determined using a reservoir simulator and it is applied as an external load to geomechanical simulator.

After some iteration in time, reservoir properties (i.e. porosity and permeability) are updated using newly determined stress, strain and displacement fields. Using this approach, Minkoff *et al*. (2003) simulated a single layer of Belridge field, California, where the initial oil in place is estimated to be 500 Mm^3 [4]. The field contains two reservoirs, one in Tulare sand and the other in diatomite layer. The Tulare sand is a shallow reservoir but the diatomite reservoir has the extension of about 305m deep, deeper than Tulare sand. The diatomite reservoir has high porosity (40%-70%) but low permeability (0.1 mD), which requires the use of hydraulic fracturing to produce economically. In their modelling, they focused on the one layer of diatomite reservoir at a depth of 361m with the initial pore pressure of 3.76 MPa. Their model extended 106m in *x* and *y* direction and 44m in *z* direction. The modified Sandler-Rubin cap plasticity constitutive model was used for the geomaterial behaviour. At the four corners of the model there were four wells. Using loosely coupled between IPARS/JAS3D after five years of production, they compared the simulations of flow separately. The results showed that using the IPARS itself the reservoir pressure changes 40% after five years of production, whereas this reservoir pressure increases to 50% for the coupled simulation. After five years of production, the surface subsidence was calculated to be 0.15m. Also, coupled simulation revealed that the permeability decreased from 0.1 to 0.001 mD.

Fredrich *et al*. (2000) carried out an investigation on surface subsidence, well casing damage and failure in Belridge diatomite reservoir, Bakersfield, California where in around 20 years of production about 1000 wells experienced casing damage [5]. Despite high thickness (about 1000 ft), porosity (45-70%) and high estimated original oil in place (about 2 billion bbl), three-quarter of the produced oil came from the overlying Tulare sand. The production from the diatomite layer was restricted, since the permeability was too low (about 0.1mD) but it improved later using hydraulic fracturing technique. The geomechanical modelling was carried out using nonlinear large deformation finite element code of JAS3D. They modelled two sections of the field: sections 33 and 29. The pore pressure determined from reservoir simulator was sent to the geomechanics simulator as an external load. The reservoir, including diatomite and porcelanit

layers, was discritized into nine layers for section 33 and ten layers for section 29. Underburden is Lower porcelanite and discritized into six elements vertically but since reported casing damage located mostly in overburden, the refinement was done within the overburden layer and was discritized into 10 elements vertically. The depth of underburden and overburden are about 2200 and 650 ft, respectively. There are also three contact surfaces in the numerical model. The models contained eight-noded Lagrangian elements. Two classes of plasticity models were used for the entire model: Drucker-Prager and generalized cap plasticity model. The former was used for the overburden and the lowermost reservoir layer and underburden and the latter for eight layers of reservoir. Three aspects of the modelling results are of particular importance: surface subsidence, deformation along vertical profiles (well damage) and changes of in-situ stress field. Surface subsidence was estimated as 7 and 5 ft for sections 33 and 29, respectively. The shear deformation was predicted to be ±0.5 ft/year.

Settari and Walters (2001) discussed the effect of coupling on the analysis of producing reservoirs [6]. They compared three types of coupling: uncoupled, partially coupling and fully coupling, explaining how partially coupling is beneficial when using the advanced reservoir and geomechanics simulators in the sense that they run separately but information is transferred between the two simulators at any certain time step. They also discussed the importance of elastoplastic constitutive models for compaction analysis. They referred to Drucker-Prager cap plasticity model and hyper-elastic nonlinear model and expressed that the first model is useful for post-failure analysis, whereas the second model is good for pre-failure analysis. Yet, both models are capable of modelling nonlinear stress-strain behaviour. Comparing the two constitutive models, they concluded that the run time of the elastoplastic model is nearly as twice as the nonlinear hyperbolic elastic model.

In this study, we developed an especial 3D FEM code which is capable of elastic analysis of porous material for elasto-plastic analysis. The main purpose was to investigate the effect of injection on plastic zone development around a porous formation. There are several commercial finite element programs available for this type of analysis; yet, neither of them is capable of being coupled with reservoir simulators. That is the objective of the developed code for coupling analysis as it supports certain predefined constitutive models. However, having access to the source code is an advantage that allows adding any other constitutive models suitable for any type of geomaterials.

The developed code was validated against some simple case studies and then was used for analysis of stress and displacements due to injection into a porous reservoir.

2. Theory of plasticity

There are many textbooks which explain the mathematical aspects of plasticity theory in detail. Below is a brief introduction to the plasticity theory. It is to be noted that most of the materials presented in this section were taken from Owen and Hinton [2].

Elaso-plastic solids behave in such a way that when stress exceeds a limited threshold (the yield stress) an irreversible straining will happen. Three basic fields of mathematical subjects are needed in order to completely cover the elasto-plastic behaviour [2]:

- explicit relationship between stress and strain for elastic condition i.e. before yielding starts;
- a yield criterion showing the stress level at which plastic flow starts; and
- stress-strain relationship for post yield behaviour.

These concepts and related aspects of plastic behaviour are explained in brief in the following sub-sections.

2.1. Elastic condition

Before plastic yielding starts the stress-strain relationship is generalized Hook's law i.e.

$$\sigma_{ij} = C_{ijkl}\varepsilon_{kl} \tag{1}$$

For isotropic material:

$$C_{ijkl} = \lambda\delta_{ij}\delta_{kl} + \mu\delta_{ik}\delta_{jl} + \mu\delta_{il}\delta_{jk} \tag{2}$$

where λ and μ are Lame's Constants and δ_{ij} is Kronecker delta.

2.2. Yield Criterion

Yield criterion describes the relationship of stresses level at which the plastic deformation starts. Generally, it is written as:

$$f\left(\sigma_{ij}\right) = k(\kappa) \tag{3}$$

where f is a function, k is a material parameter determined experimentally and κ is a hardening parameter. J_1 , J_2 and J_3 are invariant of stress field. Some yield criteria are independent of the hydrostatic pressure and, therefore, they are functions of deviatoric stress invariant J'_2 and J'_3 .The mostly used yield criteria are explained below.

The Von Mises yield criterion (1913)

This yield criterion is based on the fact that when the value of the second invariant of deviatoric stress field reaches the threshold the yielding starts:

$$\sqrt{J'_2} = k(\kappa) \tag{4}$$

The Mohr-Coulomb yield criterion

This yield criterion was first defined by Coulomb (1773) as the straight line in (σ_n,τ) space as:

$$\tau = c - \sigma_n \tan\phi \tag{5}$$

where τ is the shear stress, σ_n is the normal stress and c and Φ are cohesion and internal friction angle, respectively. It is notable that tensile stress is positive. By some mathematical manipulation, the form of yield criterion suitable for plasticity computation is driven as:

$$\frac{1}{3} J_1 \sin\phi + \sqrt{J'_2}\left(\cos\theta - \frac{1}{\sqrt{3}}\sin\theta\sin\phi\right) = c.\cos\phi \tag{6}$$

The Drucker-Prager yield criterion

This criterion is a modification of Von Mises yield criterion which is also an approximation to Mohr-Coulomb criterion. In mathematical form, this criterion is expressed as:

$$\alpha J_1 + \sqrt{J'_2} = \kappa' \tag{7}$$

in which α and k' reflect the fact that the Drucker-Prager yield criterion coincide with the outer apices of the Mohr-Coulomb hexagon and therefore are represented as:

$$\alpha = \frac{2\sin\phi}{\sqrt{3}(3-\sin\phi)} \qquad \kappa' = \frac{6c\cos\phi}{\sqrt{3}(3-\sin\phi)} \tag{8}$$

Or coincide with the inner apices of the Mohr-Coulomb hexagon, in which case are calculated as:

$$\alpha = \frac{2\sin\phi}{\sqrt{3}(3+\sin\phi)} \qquad \kappa' = \frac{6c\cos\phi}{\sqrt{3}(3+\sin\phi)} \tag{9}$$

2.3. Work hardening

After initial yielding, the yield surface may be a function of degree of plastic strain that the material has experienced.

If the yield surface does not depend on the plastic straining occurring in the material, the material is known as an elastic-perfectly plastic material. If the yield surface keeps its original shape but continues in expanding, the material is called an isotropic hardening material. Finally, if the yield surface keeps its original shape and orientation but translates in the stress space, it is known as a kinematic hardening material. In this study, we only considered elastic perfectly plastic and isotropic hardening behaviours.

The hardening parameter can be a function of the work which is done during the plastic deformation and, therefore, is said to be a work hardening phenomenon. Mathematically:

$$\kappa = W_p \tag{10}$$

where

$$W_p = \int \sigma_{ij}\left(d\varepsilon_{ij}\right)_p \tag{11}$$

If $f < k$, then the material is in the elastic domain but for $f = k$ plastic deformation initiates. After initiation of plastic behaviour, the increment change in the yield surface is dependent on the stress change:

$$df = \frac{\partial f}{\partial \sigma_{ij}} d\sigma_{ij} \tag{12}$$

Where three cases may be considered:

- if $df < 0$ it is elastic unloading and the stress state returns back inside the yield surface;
- if $df = 0$ it is neutral loading and the stress point remains on the yield surface; and
- if $df > 0$ it is plastic loading and the yield surface expands and the stress point remains on expanded yield surface.

2.4. Elasto-plastic stress-strain relationship

Outside the yield surface, the material behaviour is elasto-plastic and the strain is part elastic, part plastic. In mathematical terms, the total strain can be represented as:

$$d\varepsilon_{ij} = \left(d\varepsilon_{ij}\right)_e + \left(d\varepsilon_{ij}\right)_p \tag{13}$$

For the elastic part the stress- strain relationship is:

$$\left(d\varepsilon_{ij}\right)_e = \frac{d\sigma'_{ij}}{2\mu} + \frac{(1-2\nu)}{E}\delta_{ij} d\sigma_{kk} \tag{14}$$

where $d\sigma'_{ij}$ is the deviatoric stress field.

The plastic strain increment is a function of the *plastic potential*, Q , gradient, i.e.:

$$\left(d\varepsilon_{ij}\right)_p = d\lambda \frac{\partial Q}{\partial \sigma_{ij}} \qquad (15)$$

where $d\lambda$ is the *plastic multiplier*. The above equation is named the *flow rule*. Q , like f is a function of the deviatoric stress invariants but its determination is a very complicated experimental task. Therefore, for many cases in the field of mathematical theory of plasticity it is assumed that $f \equiv Q$ and it is named the *associated* flow rule and *normality condition* since the $\partial f / \partial \sigma_{ij}$ is normal to the yield surface.

3. 3D FEM code

We previously developed a 3D FEM program for linear elastic analysis. Here, we have expanded our program for elasto-plastic analysis, including the von Mises, Drucker-Prager and Mohr-Coulomb models. For the Von Mises model, which has hardening effect stress, the controlled mode was considered in the analysis. However, for the other two models displacement control mode was considered. Both stress and displacement control modes were integrated in the written code.

The developed 3D FEM is capable of elastic analysis of porous material for elasto-plastic analysis. It supports three dimensional isoparametric hexahedron elements with variable nodes from 8 to 20 nodes; however, in this study we used 8-noded isoparametric hexahedron. The storage method was skyline method with removing the fixed degree of freedom in order to increase the speed and decrease runtime. The solver was the Gauss elimination method based on skyline storage.

Having access to the source of the code allows coupling it with other reservoir simulators, which is a further objective of this study. Also, it enables us to integrate any other constitutive models in the analysis where is needed.

4. Validation Examples

To validate the results of our developed FEM code, in this section we present the results of some simple case studies for which the analytical solutions are available.

The first three examples consider the 8-noded unit cubic element shown in Figure 1 subjected to three sequential steps of displacements as following:

a. load step 1: +0.2 unit of tensile displacement;
b. load step 2: -0.4 unit of compression displacement; and
c. load step 3: +0.1 unit of tensile displacement.

Each step is divided into 40 sub-steps and large displacement effect is neglected. The behaviour of this cube is studied using three different constitutive models introduced in the previous sections.

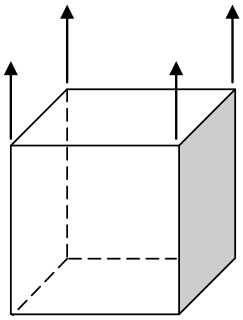

Figure 1. A unit cubic element under displacement loading

4.1. Von Mises Constitutive model

In this example, the material of the cubic element shown in Figure 1 is assumed to be elastic-perfectly plastic with hardening parameter of zero and a unit yield stress. It is also assumed to have a Young's modulus of 1.0 MPa and a Poisson's ratio of 0.3 for demonstration purposes. The material behavior under the above three loading and unloading steps is shown in Figure 2.

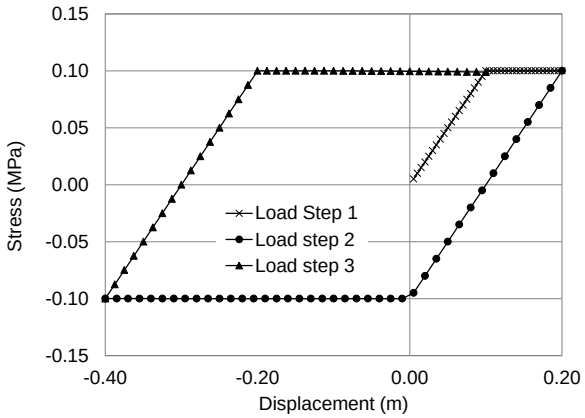

Figure 2. Material behaviour under three loading steps considering Von Mises constitutive model without hardening (perfectly plastic)

The loading path corresponding to each step is indicated in this figure. As shown in the figure, the material yields in a similar manner in both tension and compression. This is an expected result as there is no Buschinger effect for Von Mises behavior.

4.2. Mohr-Coulomb Constitutive model

In this example, the behavior of the cubic material In Figure 1 is studied when its behaviour is

assumed to be according to Mohr-Coulomb constitutive model. For computation purposes, the following material parameters are assumed for compression and tension loading modes:

$$f_c = 0.3MPa \quad (16.a)$$

$$f_t = 0.1MPa \quad (16.b)$$

$$\phi = Arc\sin\left(\frac{f_c - f_t}{f_c + f_t}\right) = 30.0 \quad (16.c)$$

$$C = \left(\frac{f_c \times f_t}{f_c - f_t}\right)\tan\phi = 0.0866MPa \quad (16.d)$$

In above equations, f_c, f_t, Φ and c are uniaxial compression strength, uniaxial tensile strength, internal friction angle and cohesion. Figure 3 presents the material behaviour under three loading and unloading steps, similar to previous example. Contrary to the previous example, the material behaves differently under tension and compression.

This is a valid result as the material yielded in a tensile stress of equivalent to 0.1 MPa and in a compressive stress of equivalent to 0.3 MPa. Since there is no hardening effect in perfectly plastic behaviour, the material yielded again at 0.1 MPa under the third loading step.

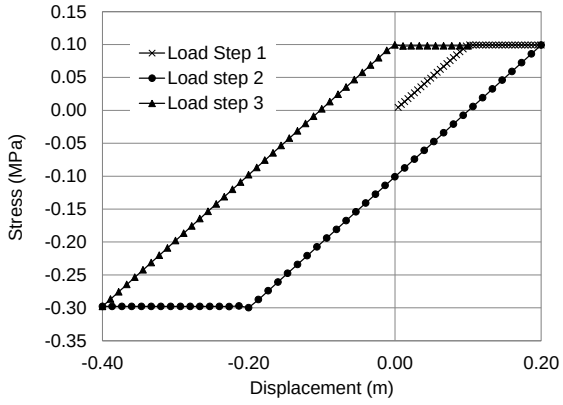

Figure 3. Material behaviour under three loading steps considering Mohr-Coulomb constitutive model

4.3. Drucker-Prager Constitutive Model

In this example, the behaviour of the cubic material in Figure 1 is studied assuming Drucker-Prager constitutive model. The input parameters to this model are (α,k') but the program uses cohesion and friction angle parameters similar to Mohr-Coulomb criteria. As explained in sub-section 2.2, there are two types of similarity between these two models: one is in tensile meridian and another in compression meridian. Figure 4 shows the material behaviour under three loading and unloading steps. The material behaviour is in such a manner that the Drucker-Prager envelope is identical to the Mohr-Coulomb envelope at the tensile meridian. Therefore, it was observed that the material yielded at a tensile stress of 0.1 MPa which is identical to that of Figure 3 under tensile loading.

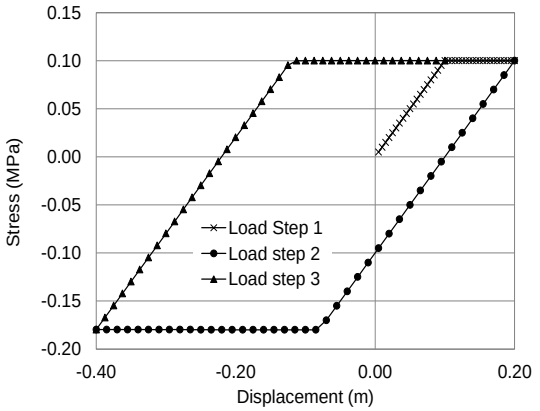

Figure 4. Material behaviour under three loading steps considering Drucker-Prager constitutive model at the tensile meridian

The resemblance of Figure 3 and Figure 4 under tensile behaviour is notable.

In Figure 5, the material behaviour is set in such a way that the Drucker-Prager envelope is identical with Mohr-Coulomb envelope at the compressive meridian. Therefore, it is observed that the material yielded at a compressive stress of -0.3 MPa which is equivalent to that of Figure 3 under compressive loading. Similarly, the resemblance of Figure 3 and Figure 5 under compressive behaviour is considerable.

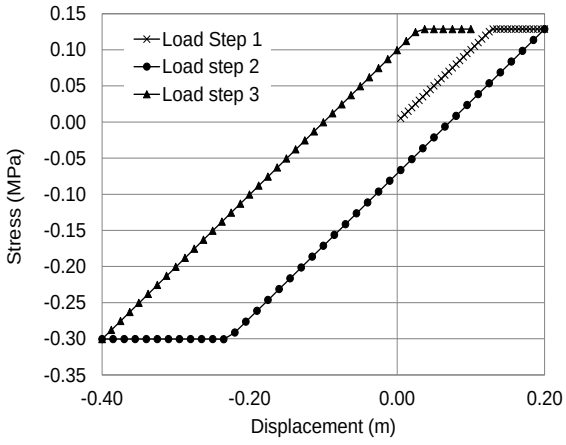

Figure 5. Material behaviour under three loading steps considering Drucker-Prager constitutive model at the compression meridian

4.4. A cylindrical hole in Mohr-Coulomb media

In this final example, we considered a cylindrical hole in a Mohr-Coulomb media. Figure 6 shows the geometry of the problem: this is a quarter of the whole model due to its symmetry.

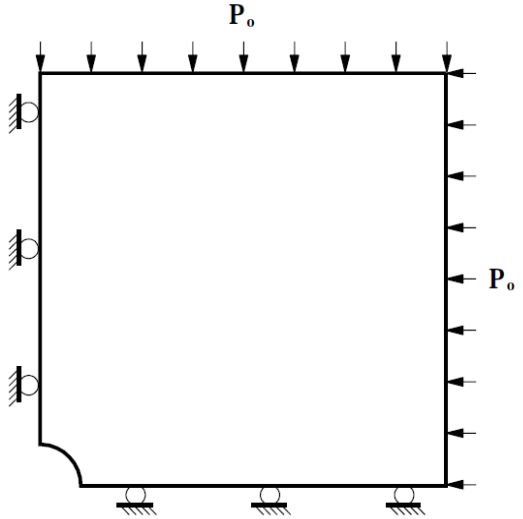

Figure 6. Model geometry of a cylinder in a Mohr-Coulomb media (after FLAC user's manual, Version 4.0, 2000)

Figure 7 presents a 2D section of the model mesh, which in fact is 3D.

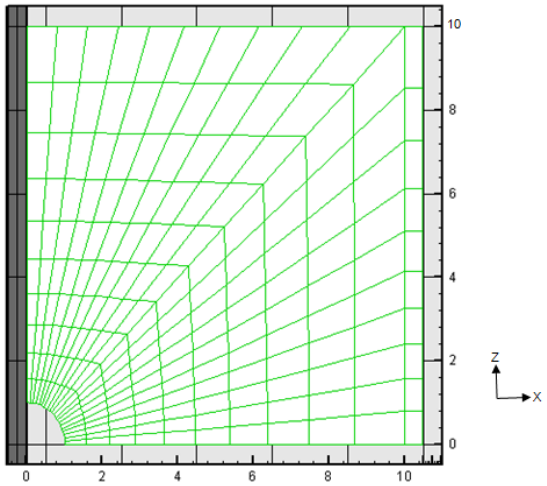

Figure 7. Mesh generated for geometry of Figure 6

The closed form solution for this problem was proposed by Salencon (1969). The plastic zone radius, R_0, is given analytically as:

$$R_0 = a\left[\frac{2}{K_p+1}\frac{P_0+\frac{q}{K_p-1}}{P_i+\frac{q}{K_p-1}}\right]^{\frac{1}{K_p-1}} \qquad (17)$$

where a is the radius of the hole, P_o is the magnitude of the initial in-situ stress, and P_i is the internal pressure inside the hole. Also,

$$K_p = \frac{1+\sin\phi}{1-\sin\phi}; \qquad (18)$$

$$q = 2c\tan\left(\frac{\pi}{4}+\frac{\phi}{2}\right). \qquad (19)$$

The radial stress at the elastic-plastic interface is:

$$\sigma_{re} = -\frac{1}{K_p+1}(2P_0 - q) \qquad (20)$$

and the radial and tangential stresses at a distance r from the center of hole within the plastic zone are:

$$\sigma_r = \frac{q}{K_p-1} - \left(P_i + \frac{q}{K_p-1}\right)\times\left(\frac{r}{a}\right)^{K_p-1} \qquad (21)$$

$$\sigma_\theta = \frac{q}{K_p-1} - K_p\left(P_i + \frac{q}{K_p-1}\right)\times\left(\frac{r}{a}\right)^{K_p-1} \qquad (22)$$

The stresses outside the plastic zone, i.e. within the elastic zone are:

$$\sigma_r = -P_0 + (P_0 - \sigma_{re})\times\left(\frac{R_0}{r}\right)^2 \qquad (23)$$

$$\sigma_\theta = -P_0 - (P_0 - \sigma_{re})\times\left(\frac{R_0}{r}\right)^2 \qquad (24)$$

The radial and tangential stresses were calculated using the above closed form solutions and also obtained from the FEM code numerically. The results are compared in Figures 8 and 9. The results show a very good agreement between the results of the two models.

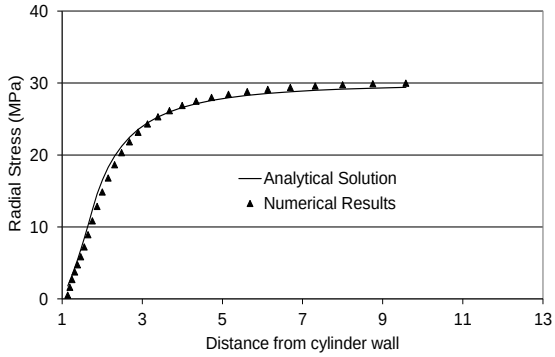

Figure 8. Comparison between FEM program and closed form solution for radial stress

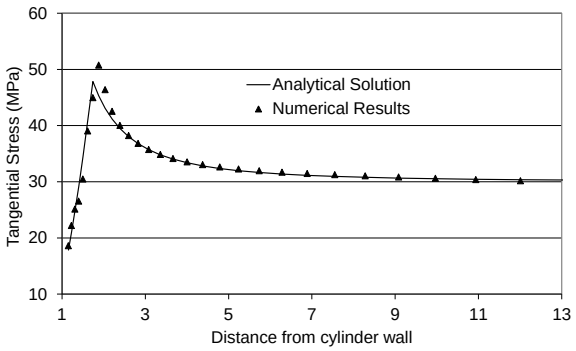

Figure 9. Comparison between FEM program and closed form solution for tangential stress and plastic zone extension

The above examples demonstrate the applicability of the developed FEM code for the plastic analysis. In the following section, the program is used to analyze the stress and strain changes due to injection into a porous zone considering elasto-plastic behavior for the formation.

5. Injection into Elasto-plastic media

A 2D section of the model in *XZ* plane at *Y*=2.0 m is shown in Figure 10. The porous formation has a rectangular cross-section in *XZ*-plane with a length of 80 m in *X*-direction, a height of 40 m in *Z*-direction and strike of several hundreds of meter aligned in *Y*-direction.

The midpoint depth of the porous formation in *Z*-direction is 500 m and the height of the porous formation is from 80.0 to 120.0 m from the bottom of the model.

In *Z*-direction, the model extends to the surface.

This allows investigating the surface-induced incidences such as probable uplift or subsidence due to reservoir injection/depletion.

The width of the porous formation in *X*-direction is from 160.0 to 240.0m from the left side of the model. The model extends 200 m in both sides (overaly 400m) in *X*-direction to ensure that it reaches to the out of the influenced zone. This model consists of 5936 nodes and 2860 isoparametric8-noded finite elements.

A formation Young's modulus of 10GPa was assumed for the porous zone in this study. This value was used in the entire model within the reservoir section and also across the overburden and underburden. This represents a moderate stiffness for the rock. The simulation started by allowing the model to consolidate under gravitational force and, then, injecting into the porous formation up to 5.6 MPa (800 psi).

In particular, we were concerned with determining the extension of the plastic zone due to injection into the porous zone.

This is important from a practical point of view in various applications of reservoir Geomechanics such as casing collapse and fracture reactivation. We performed sensitivity analysis on Cohesion assuming a constant value of 30° for the internal friction angle. The injected pressure was assumed to be 5.6 MPa which was applied at five sub steps. The iteration number to converge the model is tabulated in Table 1.

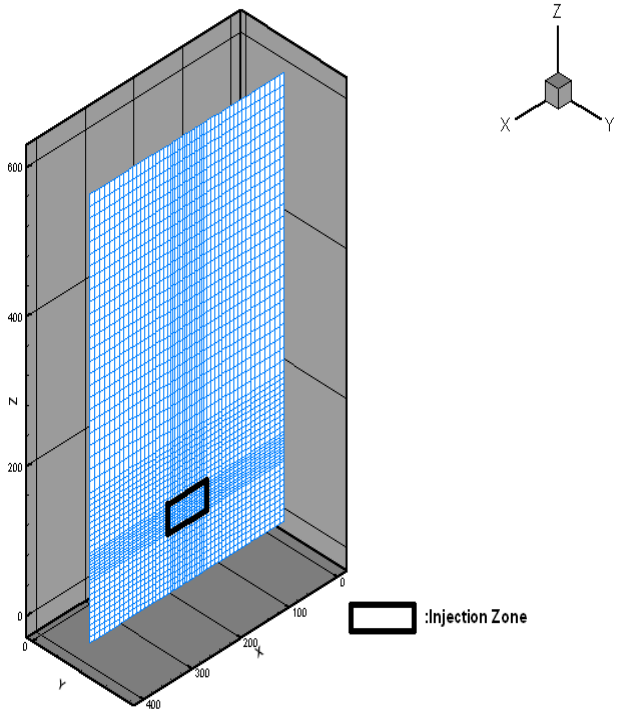

Figure 10. A 2D section in *XZ* plane at *Y*=2.0 m and the location of the injected zon

Table 1. Iterations number to convergence for each model at five different sub-steps

Cohesion (MPa)	Total Number of Iteration for each model
0.3	71
0.4	58
0.5	49
0.6	44
0.7	36
0.8	33
0.9	30
1	24
1.1	22
1.2	21
1.3	16
1.4	15
1.5	14
1.6	10

The extension of plastic zone for different values of cohesions is shown in Figure 11. The results of this figure show how the extension of the plastic zone reduces as material cohesion increases. At cohesion of approximately above 1.6 MPa, no plastic zone develops. Also, as illustrated in the figure, two spots at the corners of the injection zone are the nucleation zone for the plastic zone.

As the cohesion reduces, the plastic zone increases and at low values of cohesion the two plastic zones develop at the two sides of the porous zone intersect and generate a large plastic zone which further extends into the overburden and underburden formations. For cohesion values of smaller than 300 KPa, the model do not converge, suggesting that the degree of plastification is too high.

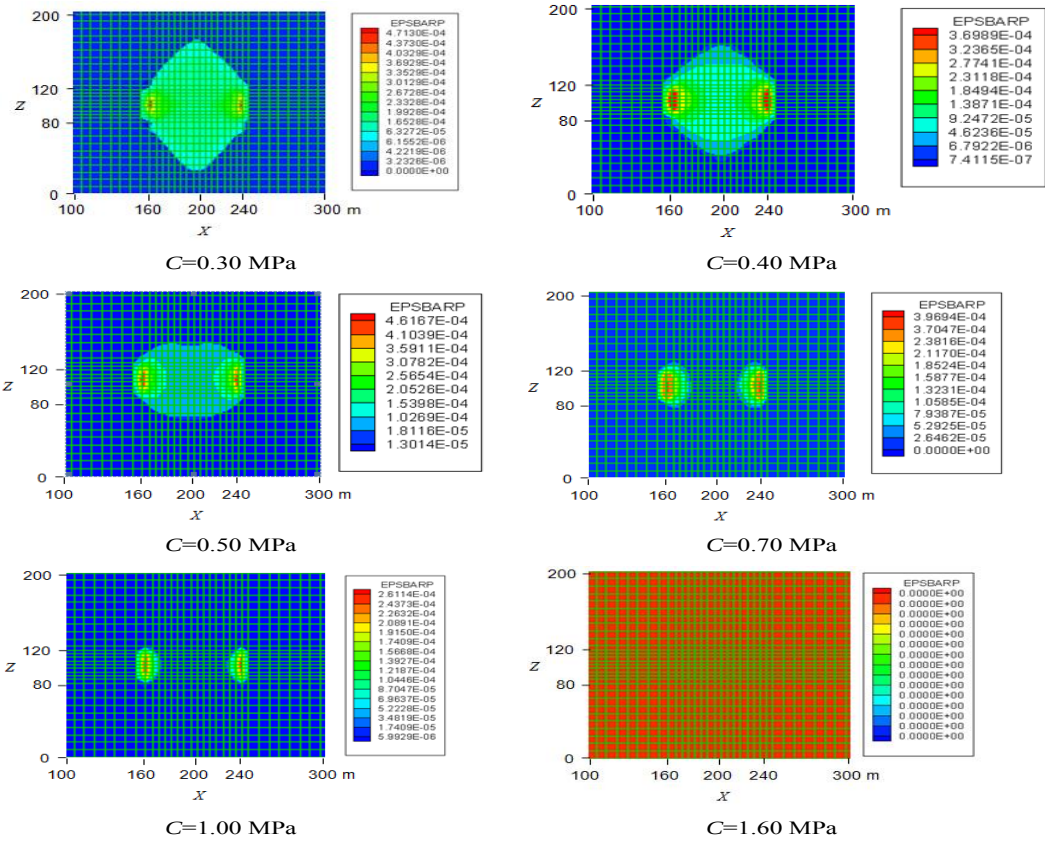

Figure 11. Reduction in plastic zone around the injected zone due to an increase in cohesion.

Conclusions

As a subsequent study to a recent one on elastic analysis of geomaterial, this study investigated the elaso-plastic behaviour of geomaterials. A 3D FEM code was developed for elasto-plasticanalysis, which can use different constitutive models. The features of the code were explained and its validity was checked by analysing some simple case studies. Comparing to elasto-plastic analysis, the elastic analysis was used to calculate the stress, displacement and strain fields, which are useful in predicting the high stress concentration zones and the direction of minor and major stresses. This information is used for wellbore stability design and to identify the propagation direction of a hydraulic fracture. However, the elastic analysis does not provide any information about failure or yielded zones. In this study, as one example, the elasto-plastic analysis was applied to study the yielded and failure zone development due to gas injection into a porous zone. The results indicated that for geomaterials with cohesion of less than 1.6 MPa the failure zones developed according to Drucker-Prager yield criterion. The lower the cohesion of the geomaterial, the larger the volume of the failure zones will be. For cohesion values of less than 300 kPa, the entire model proved to be unstable.

References

[1] *Lewis R.W., Schrefler B.A.* (1998). The Finite Element Method in the Static and Dynamic Deformation and Consolidation of Porous Media, Second Edition. Wiley, New York.

[2] *Owen D.R.J., Hinton E*. (1980). Finite Elements in Plasticity: Theory and Practice. Swansea: Pineridge Press.

[3] *Fredrich J. T., Fossum A. F.* (2002). Large-Scale Three-Dimensional Geomechanical Modeling of Reservoirs: Examples from California and the Deepwater Gulf of Mexico. Oil & Gas Science and Technology – Rev. IFP, 57, no. 5, pp. 423-441

[4] *Minkoff S.E., Stone C.M., Bryant J., Peszynska M., Wheeler M.* (2003). Coupled Fluid Flow and Geomechanical Deformation Modeling. Journal of Petroleum Science and Engineering, 38, pp. 37– 56

[5] *Fredrich J.T., Deitrick G.L., Arguello J G., de Rouffignac E.P.* (2000). Geomechanical Modeling of Reservoir Compaction, Surface Subsidence, and Casing Damage at the Belridge Diatomite Field. SPE Res. Eval. & Eng., 3, 348-359.

[6] *Settari A, Walters D.A.* (2001). Advances in Coupled Geomechanical and Reservoir Modeling with Applications to Reservoir Compaction. Society of Petroleum Engineers Journal, pp. 334-342

[7] *Itasca Consulting Group* (2000). Fast Lagrangian Analysis of Continua (FLAC) User's Guide - Version 4.0. Itasca Consulting Group, Inc. Minneapolis, Minnesota 55415 USA

[8] *Salencon, J.* (1969). "Contraction Quasi-Statique D'une Cavité a Symétrie Sphérique Ou Cylindrique Dans Un Milieu Elastoplastique," Annales Des Ponts Et Chaussées, 4, 231-236.